A Simple Model on Dislocation Dynamics

V. Koukouloyannis[1], G. Stagika[1], S. Ichtiaroglou[1], I. Groma[2], and E. Aifantis[3]

[1]*Department of Physics, University of Thessaloniki, 54006 Thessaloniki, Greece*
vkouk@skiathos.physics.auth.gr
[2]*Department of General Physics, Eötvös University Budapest,*
1518 Budapest POB. 32, Hungary
[3]*Laboratory of Mechanic and Materials, Polytechnic School,*
University of Thessaloniki, 54124 Thessaloniki, Greece

1. SUMMARY

The complete solution of the problem of the dynamical interaction of two parallel edge dislocations is obtained by a suitable transformation. Then we consider the influence of the stress field of a fixed dislocation dipole and external periodic forcing and study the generation of stable fixed points of the associated Poincaré map and the corresponding basins of attraction.

2. INTRODUCTION

Over the past decade several numerical investigations have been performed to study the dynamical properties of dislocation systems /1-8/. One of the most interesting questions stimulating these works is to understand the origin of dislocation patterning. Due to the long- range dislocation-dislocation interaction, however, the direct numerical integration of the equation of motion of a system large enough to produce patterning is extremely computation time consuming. It has recently been proposed by Bakó and Groma /9/ that the nearest neighbor dislocation interaction could be well approximated by an appropriate stochastic process. For systems containing several hundreds of dislocations it is proved numerically that the stochastic approach results in the same dynamical behavior as the "exact" integration.

The motivation of the present work is to figure out what is the minimal dislocation number, which can be well described by the above-mentioned stochastic approximation. In order to achieve this goal we have investigated, as a first approach to the full problem, the dynamical behavior of two parallel edge dislocations in the stress field of a fixed dislocation dipole under the influence of a periodic external force. Some

preliminary results of this work have been published in reference /10/.

3. INTERACTION OF TWO DISLOCATIONS

First we consider the dynamical interaction of two parallel edge dislocations assuming overdamping, which is described by the system of equations

$$\frac{dx_1}{dt} = -F(x_1 - x_2, 2), \quad \frac{dx_2}{dt} = F(x_1 - x_2, 2) \tag{1}$$

where

$$F(x, y) = \frac{x(x^2 - y^2)}{(x^2 + y^2)^2},$$

is the interaction force acting between two parallel edge dislocations having the same Burgers vector and relative position x,y, while x_1, x_2 are the horizontal displacements of the dislocations from a point, arbitrarily defined as $x = 0$ (see Figure 1). The constant vertical distance will be taken equal to $y = 2$ meaning that the distances are measured in unit half of the slip distance of the two dislocations. The dislocation mobility and the elastic constants are eliminated by introducing an appropriate unit of time.

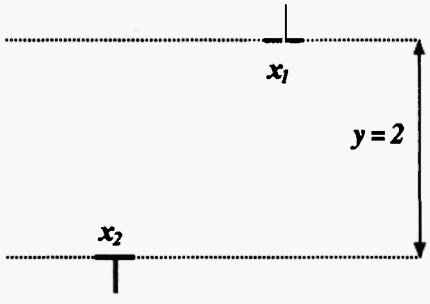

Fig. 1: Two interactive dislocations

Equations (1) are invariant under the transformation $x_1 \to -x_2$, $x_2 \to -x_1$, so that the straight line $x_1 + x_2 = 0$ is an invariant axis of symmetry, as well as under the mutual translation $x_1 \to x_1 + c$, $x_2 \to x_2 + c$, for arbitrary constant c. We perform the transformation

$$\xi_1 = x_1 + x_2, \quad \xi_2 = x_1 - x_2,$$

to equations (1), and they attain the separable form

$$\frac{d\xi_1}{dt} = 0, \quad \frac{d\xi_2}{dt} = -2F(\xi_2, y). \tag{2}$$

Equation (2a) implies that the straight lines

$$\xi_1 = x_1 + x_2 = \text{const.} \tag{3}$$

are invariant, while the solution of equation (2b) in implicit form is

$$t = -\frac{1}{2}\int \frac{d\xi_2}{F(\xi_2, y)}. \tag{4}$$

The integral in (4) can be evaluated as

$$t = -y^2 \ln\left|\xi_2^2 - y^2\right| + \frac{y^2}{4}\ln\xi_2^2 - \frac{\xi_2^2}{4} + C(y), \tag{5}$$

where $C(y)$ is an arbitrary integration constant. By putting $C(y) = -\frac{y^2}{4}\ln C'(y)$, equation (5) attains the form

$$-4t = y^2 \ln\left[\frac{C'(y)\left(\xi_2^2 - y^2\right)^4}{\xi_2^2}\right].$$

We may relate the constant $C'(y)$ to the initial condition $\xi_{20} = \xi_2(0)$,

$$C'(y) = \frac{\xi_{20}^2}{\left(\xi_{20}^2 - y^2\right)^4}\exp\left(-\frac{\xi_{20}^2}{y^2}\right).$$

With this, the solution $\xi_2 = \xi_2(\xi_{20}, t)$ is finally expressed in the implicit form

$$\frac{\left(\xi_2^2 - y^2\right)^4}{\xi_2}\exp\left(\frac{\xi_2^2}{2y^2}\right) = \left[\frac{\left(\xi_{20}^2 - y^2\right)^4}{\xi_{20}}\exp\left(\frac{\xi_{20}^2}{2y^2}\right)\right]\exp\left(-\frac{2t}{y^2}\right).$$

Equation (2b) possesses three equilibrium solutions, namely $\tilde{\xi}_2 = 0, \pm y$. The linearized equation with respect to the small variation ζ around these equilibria are, for $y = 2$, respectively

$$\frac{d\zeta}{dt} = \frac{1}{2}\zeta \qquad \text{and} \qquad \frac{d\zeta}{dt} = -\frac{1}{4}\zeta,$$

so $\xi_2 = 0$ is unstable while $\tilde{\xi}_2 = \pm 2$ are asymptotically stable. The motion on each invariant line $x_1 + x_2 - \text{const.}$ is shown in Figure 2.

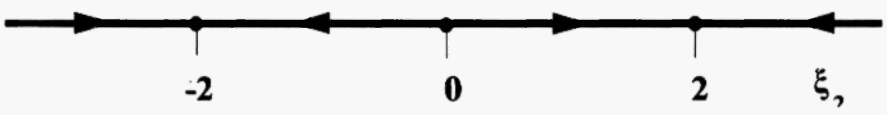

Fig. 2: The flow on an invariant line ξ_1=const.

The three equilibrium positions of the two dislocations, which correspond to the well known equilibrium dipole configurations, are shown in Figure 3. The value of the integral (3) is related to the absolute position of the pair, which is indifferent.

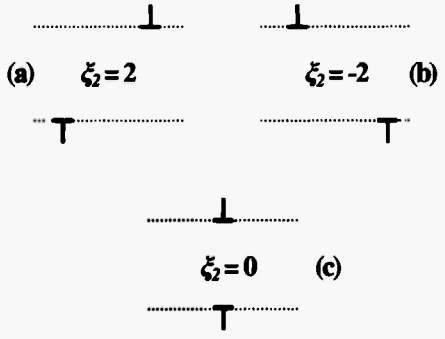

Fig. 3: The stable (a-b) and unstable (c) configurations

4. INTERACTION IN THE PRESENCE OF A FIXED DIPOLE AND EXTERNAL FORCING

In order to study the influence of other dislocations existing in the system beside the two considered above, as a simplest possible generalization an additional narrow dipole is placed in between the two dislocations (see Figure 4). The presence of the dipole, as it is expected, destroys the translational symmetry since the absolute position of the dislocations with respect to the dipole is now essential. The equations of

motion are now the following

$$\begin{aligned}\frac{dx_1}{dt} &= -\bar{F}(x_1 - x_2, 2) + m_x(t)\frac{\partial F}{\partial x}(x_1,1) + m_y\frac{\partial F}{\partial y}(x_1,1) + \varepsilon\ G(t),\\ \frac{dx_2}{dt} &= \bar{F}(x_1 - x_2, 2) - m_x(t)\frac{\partial F}{\partial x}(x_2,1) - m_y\frac{\partial F}{\partial y}(x_2,1) - \varepsilon\ G(t).\end{aligned} \tag{6}$$

The parameters m_x, m_y define the dipole strength and the term $\varepsilon G(t)$ is an external periodic forcing. As a first approximation it can be assumed that m_x also varies periodically with time, since for small enough external force, $\dot{m}_x \sim G(t)$. In this study we have selected $G(t) = \sin t$, so that $m_x = m_{x0} + d\cos t$, where m_{x0}, d and m_y are constants. Moreover, throughout this study we select $m_{x0} = m_y = 0.1$ while we consider several different values for ε, d.

When ε is different from zero, the system is non-autonomous. Its state space is the three-dimensional extended phase space (x_1, x_2, t). In order to study the dynamical behavior of the system, we use the 2π – Poincaré map G (see e.g. /11/, p. 22; /12/, p. 64). Instead of following the phase orbit for all time in the three dimensional extended phase space, we consider only the sequence of the points (x_1, x_2) at the discrete time moments $t = 2k\pi,\ k \in \wedge$. In this way, every orbit is displayed as a sequence of discrete points on the so called surface of section, which is the plane (x_1, x_2). The evolution of the system is represented by a discrete map from one point of the above sequence to the next, which is called the Poincaré map. Since the system (6) is invariant to time translations of the form $t \to t + 2k\pi$, every point of the map corresponds to a unique state of the system. A 2π-periodic orbit will be represented on the section by a fixed point of the map. Since the stable equilibria of the unperturbed system are hyperbolic, they are continued for $\varepsilon \neq 0$ to 2π-periodic orbits (e.g. /11/, p. 186), which are fixed points of the Poincaré map G.

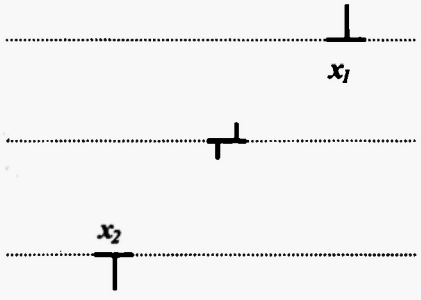

Fig. 4: The pair of the dislocations and the constant dipole

Since we will deal in the following with stable nodes, we give here the following definitions: The fixed point Q is *attracting* if there is an open neighborhood U of Q such that, for every point $P \in U$ and for every

non–negative integer n all the images of P under the map belong to the neighborhood U, i.e. $G^n(P) \in U$ and, moreover,

$$\lim_{n\to\infty} G^n(P) = Q .$$

The domain **B**, defined by all the preimages of the neighborhood U, i.e.

$$\mathbf{B} = \bigcup_{n>0} G^{-n}(U),$$

is the *basin of attraction* of Q. Let λ_1, λ_2 be the eigenvalues of the Jacobian of the map $DG(Q)$, evaluated at the fixed point Q. The point Q is a *stable node* if λ_1, λ_2 are real and

$$|\lambda_1| < |\lambda_2| < 1 .$$

A stable node is an attracting fixed point.

5. NUMERICAL RESULTS

In the following we will study the system of equations (6), for $d = 0.01$ and values of ε in the interval $0.5 \le \varepsilon < 1.3$. We will use the Poincare map and study the attracting sets of the map, which evidently prove to be only stable nodes, and their basins of attraction. The reason for that is that the system will asymptotically approach one of these sets, depending on the basin of attraction, where the initial state belongs to and, after some transient behavior, the system, for all practical purposes, will lie on that state for ever. Moreover, we will examine the domain of values $|x_i| < 10$, i.e. the maximal horizontal distance of the dislocations from the dipole will be less than 5 times the vertical distance between them.

In Figure 5, some invariant curves of the system, which support orbits of the map that end up in the four stable nodes, which are the main attracting sets of the system, are shown for $d = 0.01$ and $\varepsilon = 0.5$. These nodes are located at A: $x_1 = -1.0214$, $x_2 = -2.3896$, **B**: $x_1 = -0.5784$, $x_2 = 2.7430$, C: $x_1 = 1.5835$, $x_2 = 0.6961$ and D: $x_1 = 0.8596$, $x_2 = 4.0557$ respectively.

We may get, however, a more descriptive picture of the long–term behaviour of the system by exploring the basins of attraction of the stable nodes. In Figure 6a all four stable nodes and their basins of attraction are shown for $\varepsilon = 0.5$. The dark area on the upper right side of the figure corresponds presumably to the basin of attraction of infinity. For all orbits initially starting from this domain, both x_1 and x_2 monotonically increase and apparently tend to infinity. On the other hand, the dark area in the lower left side is the basin of attraction of another stable node E: $x_1 = -11.7687$, $x_2 = -8.70386$, which is not shown in the figure since we want to concentrate in the central area of the section. In this and the following figures, the various tones of gray in a

basin of attraction visualize the rate of convergence to the corresponding node. Between two consecutive tones of gray there is a time difference of 1000 periods for convergence to the fixed point of the corresponding basin of attraction with an accuracy of 10^{-4}.

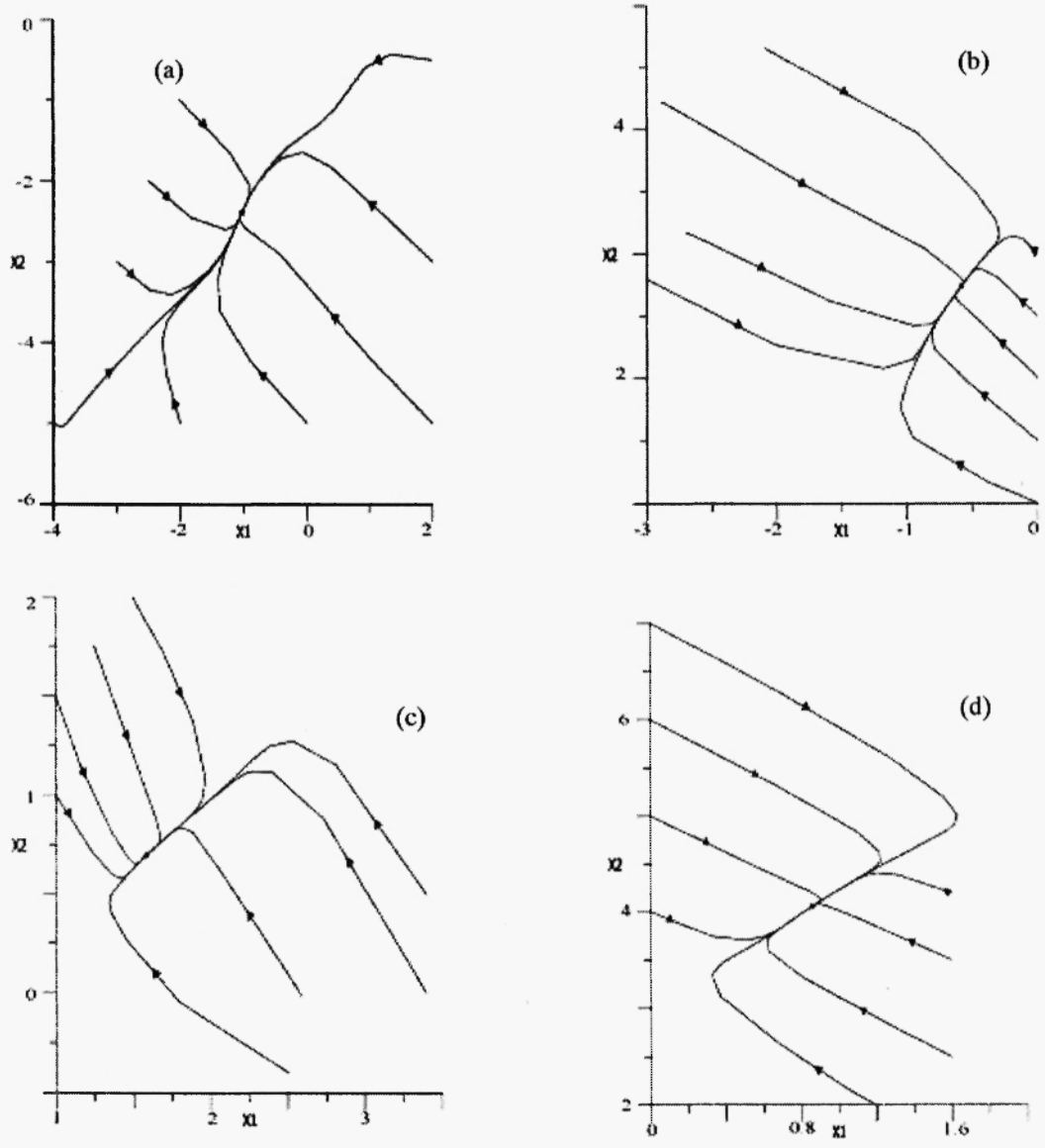

Fig. 5: Some invariant lines of the Poincaré map for $d = 0.01$ and $\varepsilon = 0.5$.

For $\varepsilon = 0.6$ we observe in Figure 6b that the stable node C has disappeared, presumably by colliding with a saddle point and performing an inverse saddle-node bifurcation, while its basin of attractions unites with

this of point A. Another stable node appears however for $\varepsilon = 0.7$ (Figure 6c), which also disappears for $\varepsilon = 0.8$ (Figure 6d), but this time its basin of attraction unites with the one of point B. At the same time, the basin of attraction of ∞ considerably shrinks. In these two last figures it is worth noting the invasion of the basin of point A between those of point B and ∞.

For still larger values of $\varepsilon = 0.85$ to 1.3, there is a multitude of bifurcations, as can be seen in Figures 6e-f and 7a-d. New stable nodes appear and disappear, while the basins of ∞ and E have altogether disappeared from the domain shown in the figures. For still larger values of ε, the situation depicted in Figure 7d seems to remain structurally stable and no more bifurcations occur up to $\varepsilon \sim 2$.

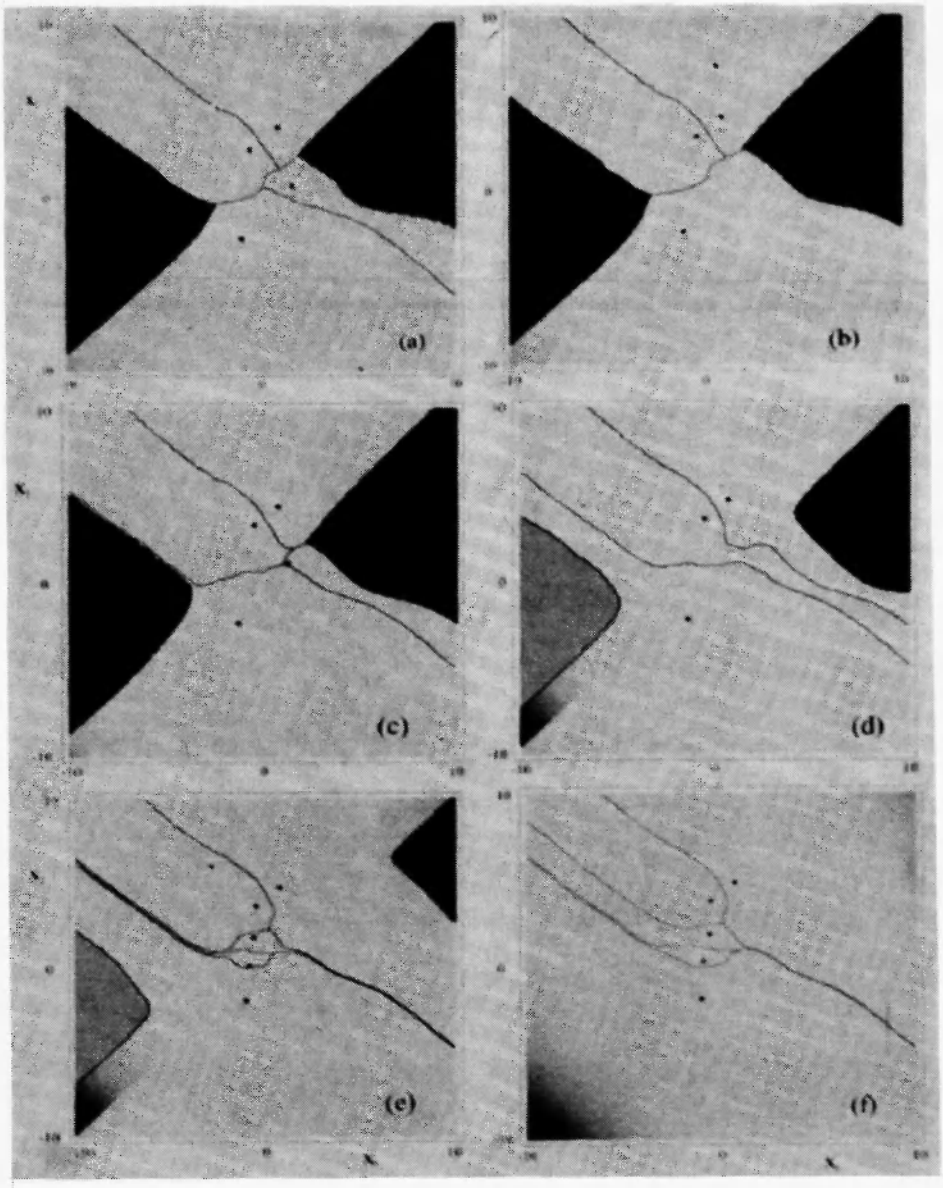

Fig. 6: The stable nodes and their basins of attraction for $d = 0.01$ and (a) $\varepsilon = 0.5$, (b) $\varepsilon = 0.6$, (c) $\varepsilon = 0.7$, (d) $\varepsilon = 0.8$, (e) $\varepsilon = 0.85$ and (f) $\varepsilon = 0.9$

Note that in some of the figures there are narrow zones of a basin of attraction of some point, separating two other basins of different fixed points. This fact means that a slight variation of the initial conditions may result in a totally different asymptotic behavior of the system. Note that in the area of these zones, this sensitivity exists, although the system is not intrinsically chaotic.

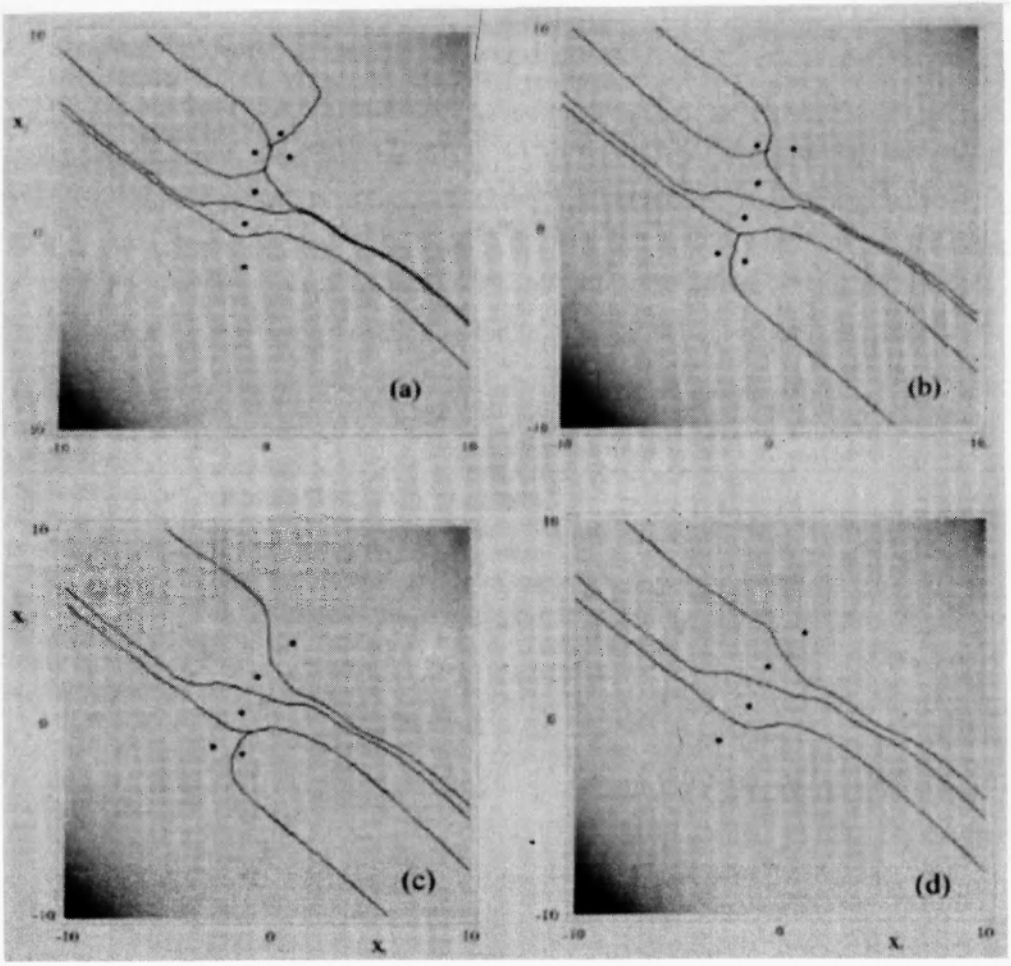

Fig. 7: Stable nodes and their basins of attraction for $d = 0.01$ and (a) $\varepsilon = 1$, (b) $\varepsilon = 1.1$, (c) $\varepsilon = 1.2$, (d) $\varepsilon = 1.3$.

6. CONCLUSIONS

The dynamical properties of a system of the two mobile dislocations and an immobile dislocation dipole are studied under periodic external force. With increasing external force amplitude the dislocation ensemble studied shows more and more complex behavior, signaled by the nucleation of new "dynamics" fixed points,

up to $\varepsilon \sim 1$. However, the system does not exhibit chaotic behavior. This can be attributed to the fact that all the stable fixed points are strongly attracting nodes, causing the asymptotic manifolds of the saddle points to bend and preventing them from intersecting.

ACKNOWLEDGEMENTS

This work has been supported by the scientific program PENED-1999, "Gradient theory, stochasticity and self-organization", No 1958/100164, Greece and the OTKA program of the Hungarian Academy of Science under tContract No 043519. The support of EC under the RTN–DEFINO project No. HPRN-CT-2002-00198 is acknowledged. The support of a Greek-Hungarian cooperative research project, which made possible I. Groma's visit to A.U.T. and visits of the Greek authors to Eötvös University, is also acknowledged.

7. REFERENCES

1. A. Gullouglu, D. Srolovity, R. LeSar, and P. Lomdahl, *Scr. Metall.* **23**, 1347 (1989).
2. R.J. Amodeo and N.M. Ghoniem, *Phys. Rev. B* **41** 6958 (1989)
3. V.A. Lubarda, J.A. Blume, and A. Needleman, *Acta Metall.* **41**, 625 (1993)
4. X.F.Fang and W. Dahl, *Mater. Sci. Eng. A* **164**, 300 (1993)
5. I. Groma and G.S. Pawley, *Mater Sci. Eng. A* **164**, 1459 (1993)
6. Y.J. Bréchet. G.R. Canova, and L.P. Kubin, *Scr. Metall. Mater.* **29**, 1165 (1193)
7. B. Devince and M. Condat, *Acta Metall. Mater.* **40**, 2629 (1992)
8. I. Groma, *Phys. Rev. B*, **56**, 5807 (1997)
9. B. Bakó and I. Groma, *Phys. Rev. B*, **60** 122 (1999)
10. G. Stagika, S. Ichtiaroglou, F.F. Csikor, I. Groma and E. Aifantis, *Int. J. Mech. Behavior of Materials* **14**, 1 (2003)
11. J. Guckenheimer and P. Holmes, *Nonlinear Oscillations, Dynamical Systems, and Bifurcations of Vector Fields*, Springer-Verlag, New York, 1983.
12. S. Wiggins, *Introduction to Applied Nonlinear Dynamical Systems and Chaos*, Springer-Verlag, New York, 1990.